

# Poly(ethylene oxide)/Laponite nanocomposites via melt-compounding: effect of clay modification and matrix molar mass

Wendy Loyens, Patric Jannasch, Frans H.J. Maurer\*

*Department of Polymer Science and Engineering, Lund Institute of Technology, Lund University, P.O. Box 124, SE-221 00 Lund, Sweden*

Received 21 June 2004; received in revised form 31 October 2004; accepted 22 November 2004

Available online 15 December 2004

## Abstract

The present study focuses on the preparation of poly(ethylene oxide) (PEO) nanocomposites based on the synthetic Laponite clay. The clay was added both in its pure form as well as organically modified with low molar mass poly(ethylene glycol) (PEG) components in order to enhance the compatibility between Laponite and PEO. Several PEG's with different end groups were used. Almost all of them were found to intercalate in the clay intergallery spacing. An order of intercalation efficiency could be established. The modified clays displayed a good thermal stability at the nanocomposite processing temperature.

The nanocomposites based on the pure Laponite clay as well as the modified clays display an intercalated structure with a modest intergallery spacing. The ion-dipole modification with the PEG's was ineffective in improving the compatibility between PEO and the Laponite silicate layers. Their respective mechanical properties were found to be increased a little, which can be attributed to the low effective aspect ratio of the silicate platelets present in the nanocomposites. This is caused by the low initial aspect ratio of Laponite ( $w/t=25$ ) and the limited basal spacing increase. The addition of clay does not result in nucleation of the PEO crystallisation. In contrast, the crystallisation was inhibited, resulting in decreased heat of fusions, especially for the pure Laponite nanocomposites. The nanocomposites based on the modified Laponites display a good thermal stability.

© 2004 Elsevier Ltd. All rights reserved.

*Keywords:* Clay nanocomposites; PEO; Laponite

## 1. Introduction

Poly(ethylene oxide) (PEO)/clay nanocomposites offer new promising materials which display a great potential for use in various application fields [1–6]. The hydrophilic nature of PEO presents an important advantage when preparing intercalates of PEO and hydrophilic silicate clay platelets. In a previous publication [4], we reported the preparation by melt-extrusion and characterisation of various PEO/clay nanocomposites, based on several commercially available Cloisite clays.

There exist a large number of other clay types with their own typical characteristics, besides the very often studied montmorillonite (Cloisite) clays. Laponite® is an entirely synthetic clay with a trioctahedral smectite structure. The

clay platelets have a disc-like shape with an aspect ratio ( $w/t$ ) of 25. Due to this relatively small aspect ratio, preferential orientation is less likely to occur [3] which can be beneficial for isotropically sensitive properties. Laponite presents the additional advantages of having a high structural regularity and a low level of impurities, which is beneficial for impurity (metal) sensitive properties, like ion conductivity [3,7]. The excess negative charge, originating from a non-stoichiometric cation substitution in the crystal structure, is compensated by the presence of  $\text{Na}^+$  ions in the intergallery spacing between the silicate layers [7]. Literature reports on polymer nanocomposites based on Laponite are mainly focussed on direct polymerisation [8] and solution preparation [3,7,9] techniques. This is motivated by the excellent dispersability of Laponite in water.

Our previous publication [4] and various reports in literature [2,10–13] proved the ability of PEO to form intercalates with natural montmorillonite clay (Cloisite

\* Corresponding author. Tel.: +46 46 222 9149; fax: +46 46 222 4115.  
E-mail address: [frans.maurer@polymer.lth.se](mailto:frans.maurer@polymer.lth.se) (F.H.J. Maurer).

Na<sup>+</sup>). However, a satisfying increase of the mechanical properties, often envisaged when preparing polymer/clay nanocomposites, usually requires highly intercalated (high basal spacing increase) or even exfoliated nanostructures [4, 14–16]. The use of organically modified clays is often essential to improve the compatibility between the polymer and the silicate layers. There exist two main preparation routes to obtain organically modified clays. The most commonly used method is based on ion exchange of the cations present in the intergallery spacing (e.g. Na<sup>+</sup>) with organic cations, very often bulky quaternary ammonium ions [17,18]. On the other hand, it is also possible to prepare organoclays via an ion-dipole interaction [19]. This usually involves the intercalation of non-ionic, low molar mass components, which show a strong chemical compatibility with the intercalating polymer. The originally present small cations remain located at the surface of the silicate layers. Ishida et al. [19] reported on the modification of a bentonite clay with hexadecylamine. They studied the modifier conformation and its thermal properties as a function of the modifier concentration. Several authors have studied the conformation of modifier chains in confined spaces [17,18], relevant for the optimisation of nanocomposite properties.

The scope of the present study is twofold. The first section is dedicated to the organic modification of the Laponite clay with low molar mass poly(ethylene glycol)'s (PEG). The main difference between the PEG's is the chemical nature of their respective end groups. The modified clays are characterised with small-angle X-ray scattering (SAXS), differential scanning calorimetry (DSC) and thermal gravimetric analysis (TGA). The second part of the paper deals with the characterisation of the actual PEO nanocomposites, based on the pure Laponite clay and several selected organically modified Laponite clays. They have been prepared according to a melt extrusion process. Their nanostructure, mechanical response and thermal behaviour are examined. The effect of the silicate concentration, modification (modifier concentration) and matrix molar mass is evaluated.

## 2. Experimental

### 2.1. Materials

Two commercial grades of PEO, with a respective molar mass of 100,000 g/mol (LMW) and 300,000 g/mol (HMW), were purchased from Aldrich. The pure Laponite clay (Laponite<sup>®</sup> RD) was kindly donated by Southern Clay Products. Its cation exchange capacity (CEC) is 60 mequiv./100 g clay. The organic modification was performed with low molar mass poly(ethylene glycol) (PEG) components, which are used as received. Their characteristics are presented in Table 1. The PEO grades and the clays were dried before use.

Table 1  
Characteristics of the used organic modifiers

Modifier	Denotation <sup>a</sup>	Supplier	Molar mass (g/mol)
4,7,10-Trioxa-1,13-tridecanediamine	A/a	Aldrich	220.3
Poly(ethylene glycol)	B/b	Aldrich	200
Poly(ethylene glycol)methyl ether	C/c	Ega Chemie	350
Poly(ethylene glycol)bis(carboxymethyl)ether	D/d	Aldrich	250
Tetraethylene glycol dimethyl ether	E/e	Aldrich	222.3

<sup>a</sup> Capital letter=modification at 120 °C, small letter=modification at room temperature.

### 2.2. Clay modification

The clay modification was performed according to a melt annealing procedure [19]. Pure Laponite clay was physically mixed with the different organic PEG modifiers at room temperature after which the mixtures were left to anneal under a nitrogen purge at a controlled temperature during 1 h. The modification procedure was performed both at an elevated temperature (120 °C) as well as at room temperature (25 °C) and the modifier concentration was based on the CEC of Laponite (e.g. 1 CEC, 2 CEC or 3 CEC). The respective weight percentage of modifier present in the modified Laponite clay is given in Table 2 and is based on the molecular weight of the modifier. The modified Laponite clays were characterised with SAXS, DSC and TGA, as described in the respective experimental sections.

### 2.3. Melt-compounding

The nanocomposites were prepared in a two-step melt-compounding procedure. Their composition is based on the effective weight percentage of the clay silicate, providing a modifier independent basis for comparison. Firstly, a PEO/silicate masterbatch, based on 10 wt% silicate, was compounded using a Brabender batch mixer at 120 °C, 40 rpm during 8 min. In the second compounding step, the masterbatch was diluted with neat PEO using a co-rotating twin screw midi-extruder at 120 °C (150 °C for HMW PEO), 80 rpm during 10 min. The use of a recirculation channel allows the extruder to be operated as a batch mixer. The silicate content was varied between 0 and 5.0 wt%. After melt mixing, the nanocomposites were compression moulded into 1 mm thick samples at 120 °C, and left to cool to room temperature. Before characterisation, the samples were dried overnight at 40 °C and kept in a dessicator until measurement.

### 2.4. Small angle X-ray scattering (SAXS)

Structural information is gathered from SAXS

Table 2

Weight percentage of organic modifier present in the respective modified Laponite clay based on the CEC of Laponite and the molecular weight of the respective modifier

	Lap-mod A/a (wt%)	Lap-mod B/b (wt%)	Lap-mod C/c (wt%)	Lap-mod D/d (wt%)	Lap-mod E/e (wt%)
1 CEC	11.7	10.7	17.1	13.0	11.9
2 CEC	20.9	19.3	29.3	22.9	20.6
3 CEC	28.4	26.3	38.9	31.1	28.5

experiments. They were performed with a Kratky compact camera equipped with a linear position sensitive detector (OED 50M from MBraun, Graz). A Seifert ID 3000 X-ray generator provides the Cu  $K_{\alpha}$  radiation with a wavelength of 1.542 Å. The samples were placed in a sealed solid sample cell between mica sheets and measured during 1 h at 25 °C.

### 2.5. Differential scanning calorimetry (DSC)

Differential scanning calorimetric measurements were performed using a TA Instruments Q1000 DSC. The thermal transitions of the modifiers and the respective modified clays were characterised during a single heating run. Therefore, the samples were sealed in a hermetic pan and quenched to  $-80$  °C, followed by the heating run up to 130 °C at a heating rate of 5 °C/min. The nanocomposites were characterised according to a multiple scanning profile. A first heating run was conducted from room temperature to 120 °C, followed by a cooling run down to  $-70$  °C. The second heating run was performed from  $-70$  to 120 °C. The heating/cooling rate was 10 °C/min.

### 2.6. Thermogravimetric analysis (TGA)

Determination of the thermal stability of the materials was done with a TA Instruments Q500 TGA. The thermal decomposition of the modified clays was evaluated from a high resolution dynamic scan (resolution: +5) at a heating rate of 50 °C/min from 30 to 550 °C. This implies that the continuous heating of the sample is halted as soon as the onset of a transition is detected. The heating continues when the transition is completed. The TGA characterisation of the nanocomposites was performed according to a custom mode from 40 to 900 °C at a heating rate of 10 °C/min.

### 2.7. Dynamic mechanical properties (torsion pendulum)

The dynamic mechanical properties in shear of the nanocomposites were determined using a torsion pendulum ATM3 Myrenne apparatus. The experiments were performed in the temperature range  $-90$  to 30 °C at a heating rate of 2 °C/min and a frequency of 1 Hz. The samples had a thickness of 1 mm, a width of 9 mm and a measuring length of 50 mm.

## 3. Results and discussion

### 3.1. Organic modification of Laponite clay

#### 3.1.1. Structural characteristics

The effectiveness of the performed organic modification, as described in the experimental section, is evaluated from the SAXS diffraction spectra of the respective modified Laponite clays. Fig. 1(a) and (b) presents the spectra for the

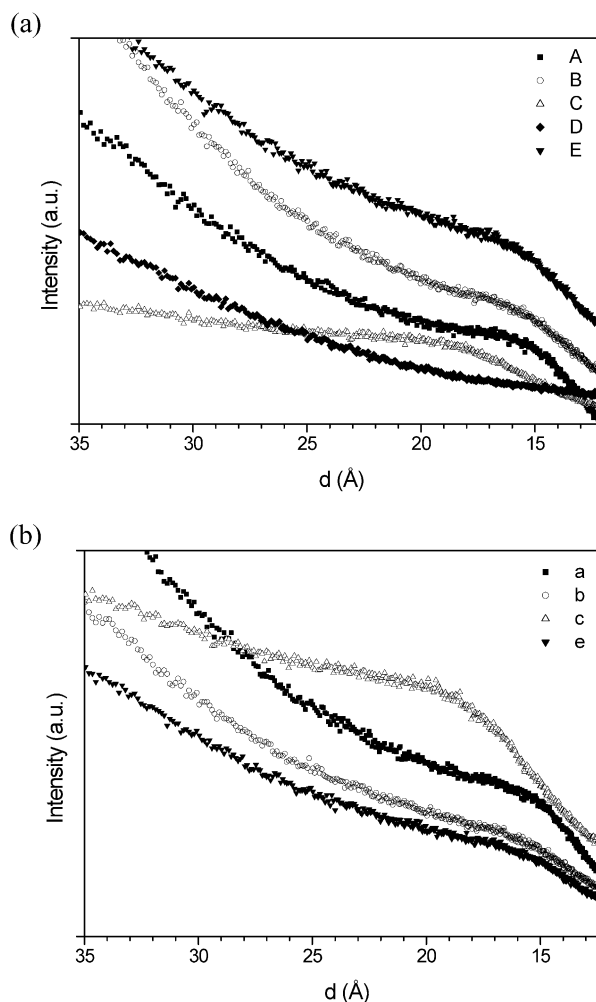


Fig. 1. SAXS diffraction spectra of the various Laponite clays modified at 120 °C (a) and at room temperature (b), with a modifier concentration equal to 2 CEC of the pure Laponite clay. The lettering refers to the notation presented in Table 3, where a capital letter denotes the modification performed at 120 °C and the small letter denotes room temperature. The curves have been shifted along the Y-axis for clarity.

modifications performed at elevated temperature (120 °C) and at room temperature (25 °C), respectively. The figure represent the clays modified with a modifier concentration equal to two times the CEC of the pure Laponite clay (2 CEC). A capital letter denotes the clays modified at 120 °C, while a small letter refers to clays modified at 25 °C. The basal spacing of pure Laponite is commonly located at 10 Å (data measured but not shown).

Upon comparing the SAXS spectra, it can be concluded that the proper temperature of modification appears to be of minor importance. The corresponding modified clays display similar spectra, regardless of the temperature. On the other hand, the modifier is found to have a more profound influence on the modified clay characteristics. Nearly all modifiers reveal the ability to intercalate between the silicate layers, resulting in an opening of the intergallery space. This is reflected by a distinct increase of the basal spacing compared to pure Laponite. The observed diffraction peaks show a significant broadness, which can be attributed to the presence of a wide variety of basal spacings within the same modified clay. Only poly(ethylene glycol)-bis(carboxy methyl)ether (D/d) does not appear to intercalate as no increase of the basal spacing could be detected, regardless of the modifier concentration.

Fig. 2 shows the effect of the modifier concentration for the Laponite clay modified with component C/c at 25 °C. It is obvious that a modifier concentration equal to 1 CEC is insufficient to detect a clear diffraction peak. Increasing the modifier concentration increases the basal spacing, although the difference between a modifier concentration equalling 2 CEC ( $d=19.3$  Å) and 3 CEC ( $d=19.6$  Å) is only minor. A similar trend is also observed for the other modified clays. The strongest increase in basal spacing is obtained when using poly(ethylene glycol)methyl ether (C/c) as the modifier. Based on the diffraction peak maximum for clays modified with a modifier concentration equalling 2 CEC, the following order of intercalation efficiency can be presented: poly(ethylene

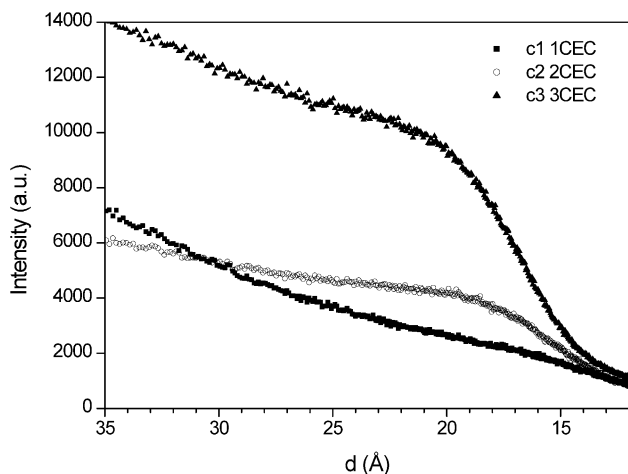


Fig. 2. SAXS diffraction spectra of the Laponite clay modified with various concentrations of modifier C/c (poly(ethylene glycol)methyl ether) at 25 °C.

glycol)methyl ether (C/c) ( $d=19.3$  Å) > tetraethylene glycol dimethyl ether (E/e) ( $d=17.2$ ) > 4,7,10-trioxa-1,13-tridecanediamine (A/a) ( $d=16.6$ ) > poly(ethylene glycol) (B/b) ( $d=15.2$  Å) > poly(ethylene glycol)bis(carboxy methyl) ether (D/d).

### 3.1.2. Thermal properties

Fig. 3 presents the DSC results of the pure modifiers measured during the described first heating run (see Section 2). All modifiers display thermal transitions well below room temperature.

DSC measurements of the prepared modified clays reveal the effect of the modifier intercalation on its thermal transitions. Figs. 4 and 5 present the DSC first heating measurements of the clays modified with various concentrations of component A (at 120 °C) and component c (at 25 °C), respectively. Pure modifier A/a shows a cold crystallisation peak followed directly by the melting endotherm. The modified Laponite clays no longer display any clear thermal transitions. The response of the clays modified with component C/c is similar. The pure modifier has a clear melting behaviour at low temperatures, revealing its ability to crystallise. The respective modified Laponite clays, however, no longer display clearly detectable transitions, although a very minor (melt) transition around  $-20$  °C can be seen for the 3 CEC modified clay. The other modified clays display a similar behaviour. It seems permitted to attribute the lack of thermal transitions to the intercalation of the modifier chains in the intergallery spacing.

Based on several literature reports [17,18] and our experimental results, it is possible to extract information concerning the actual conformation of the modifier chains in the intergallery spacing. The basal spacings achieved upon modification ( $\Delta d=5.2$ – $9.6$  Å), indicate the presence of two different modes of modifier conformation. A first group (modifiers A/a, B/b and E/e) only shows a moderate improvement ( $\Delta d \cong 5.2$ – $7.2$  Å) whereas modifier C/c results in a more distinct basal spacing increase of 9.3–9.6 Å. In

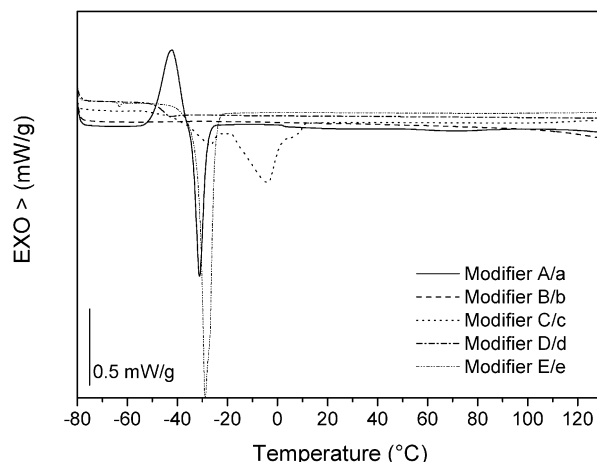


Fig. 3. DSC heating curves of the pure modifiers.

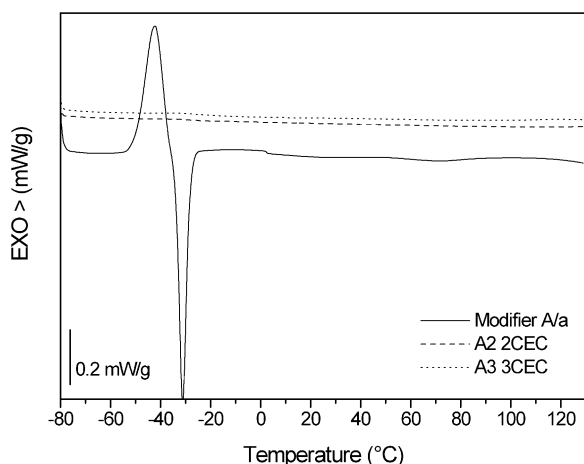


Fig. 4. DSC heating curves of modifier A/a and its respective Laponite clays modified at 120 °C with a modifier concentration equal to 2 (A2) and 3 CEC (A3).

literature, the former increase is commonly associated with the presence of a 'bilayer' conformation of the organic modifier. This means that the chains are present in an aligned position parallel to the clay surface consequently inhibiting the formation of modifier crystal structures. The actual number of C and O atoms present in the main chain can be calculated to be around 12–15. This is highly comparable to the number of C atoms present in the alkyl ammonium chain, for which this conformation has been detected and even simulated [17,18]. Ishida et al. [19] also proved the presence of a bilayer modifier structure when performing an ion-dipole interchange of a bentonite clay using hexadecylamine (C = 16) as the modifier. In contrast to our system, they established a higher basal spacing increase when increasing the modifier concentration to 3 CEC. When considering modifier C/c, it is important to note that its molar mass is substantially higher compared to the others (Table 1). This is the main reason for the higher

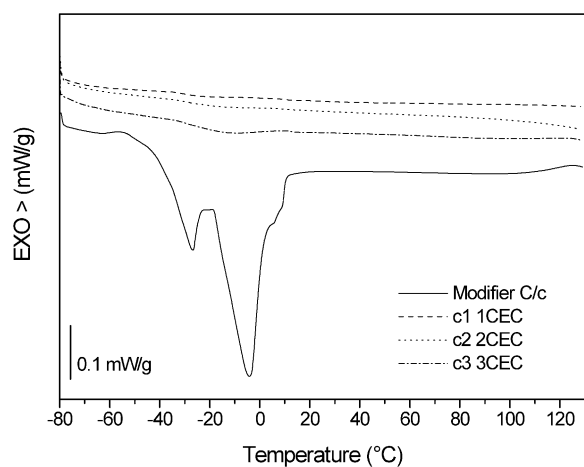


Fig. 5. DSC heating curves of modifier C/c and its respective Laponite clays modified at 25 °C with a modifier concentration equal to 1 (c1), 2 (c2) and 3 CEC (c3).

increase in basal spacing achieved for this modifier. The number of C and O atoms is approximated to be around 22. It has been shown that both an increase of the number of C atoms in the modifier (alkylammonium) chain [17,18] as well as increasing the modifier concentration (i.e. (CEC) [19] leads to a distinct increase of the intergallery spacing. This increase was found to be stepwise rather than linear. However, an 'intermediate' conformation can be obtained when the length of the intercalant is causing an excess density leading to a spreading of the silicate layers. The accommodation of a new layer implies sufficient spacing equalling the diameter of a CH<sub>2</sub> group. If the actual basal spacing is smaller, the accommodation of this new layer is unlikely. The actual intercalated chains are basically spreading the existing layers but do not create a totally new conformation. [18]. It now seems reasonable to conclude that the actual conformation of the modifier C/c is pending between a 'bilayer' and a 'trilayer' or paraffin-type of organisation [18,19]. The broadness of the diffraction peak would suggest such a transition state [18].

### 3.1.3. Thermal stability

A crucial point for any organically modified clay is the thermal stability of the used modifier in view of the use in a consecutive melt extrusion processing step. Although our modified Laponite clays are melt extruded with PEO at a relatively low temperature (120 °C), it is important to examine their decomposition behaviour. Fig. 6 presents the TGA curves of the pure modifier A/a; C/c and E/e as they show the best potential use in PEO nanocomposites. At the proposed processing temperature, the modifiers show no significant degradation. Their onset temperature of decomposition is sufficiently high compared to the actual processing temperature.

Fig. 7 presents the TGA curves of pure Laponite and various organically modified (2 CEC) clays. Pure Laponite shows an initial weight loss at relatively low temperatures. This can be assigned to loss of intercalated water, although

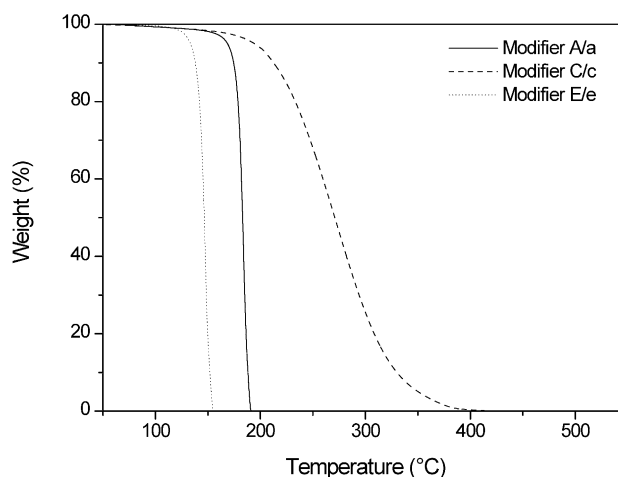


Fig. 6. TGA curves of the pure modifiers.

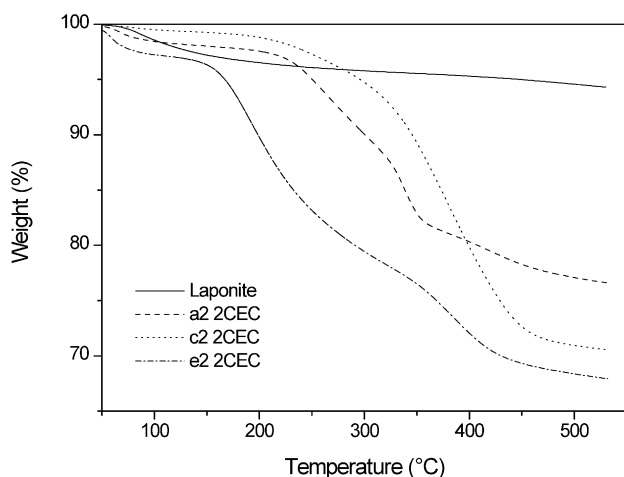


Fig. 7. TGA curves of pure Laponite and Laponite modified with 2 CEC of modifier A/a (a2 2CEC); C/c (c2 2CEC) or E/e (e2 2CEC) at 25 °C, respectively.

the samples were dried before measuring. The organic modification nearly eliminates this initial weight loss. Especially the clay modified with modifier C/c reveals a stable structure with a high onset temperature of decomposition. At the processing temperature of 120 °C, the thermal stability of the modified clays is sufficiently high.

### 3.2. PEO/(pure/modified) Laponite nanocomposites

#### 3.2.1. Structural characteristics

The PEO/clay nanocomposites were prepared via melt extrusion. Subsequent compression moulding provided samples for the various characterisation techniques. Firstly, Fig. 8(a) and (b) presents the SAXS diffraction spectra of the PEO/pure Laponite nanocomposites for the LMW and the HMW PEO, respectively. Table 3 provides the basal spacing of the different PEO nanocomposites derived from the SAXS peak maximum. As mentioned earlier, the diffraction peak of the pure Laponite clay is located at 10 Å. From Fig. 8(a) and Table 3, it follows that the LMW

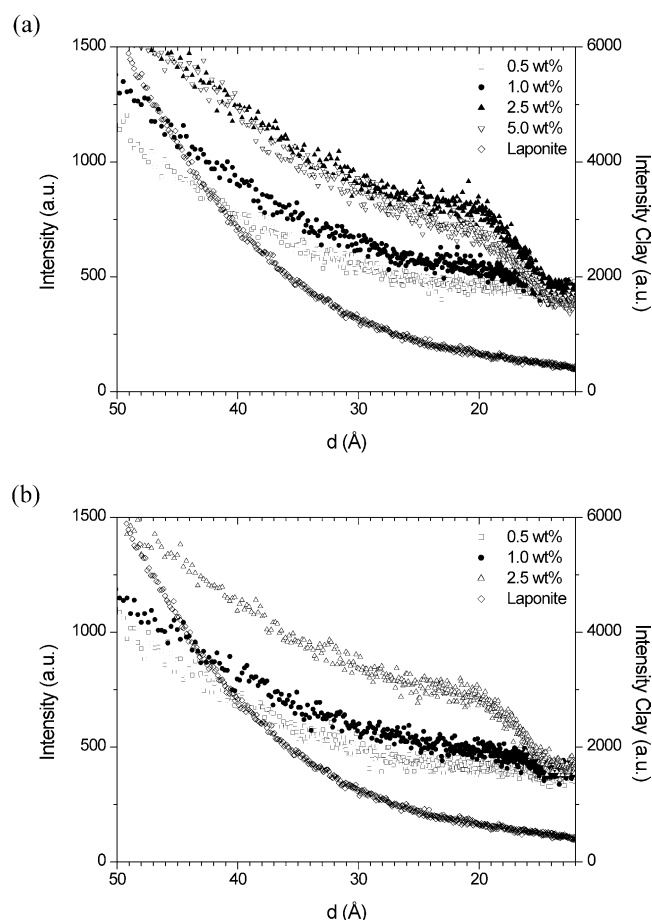


Fig. 8. SAXS diffraction spectra of the PEO/(pure) Laponite nanocomposites for the LMW (a) and HMW (b) PEO material.

PEO/Laponite nanocomposites display a clear diffraction peak situated around 18–19 Å, depending on the silicate concentration. Hence, PEO clearly demonstrates the ability to intercalate between the Laponite silicate layers. The actual basal spacing increase is rather limited, in close similarity to the earlier studied PEO/Cloisite Na<sup>+</sup> nanocomposites [4]. Similar observations have also been

Table 3

Basal spacing of the PEO nanocomposites as a function of the matrix molecular weight for the different Laponite clay types and silicate concentrations. The basal spacing of the respective pure clay is given as a reference

Silic. conc. (wt%)	Laponite RD		Modifier a	Modifier c	Modifier e
	LMW	HMW	LMW	LMW	LMW
Pure clay	10	10	16.6	19.3	17.6
0.5	16.8	<sup>a</sup>	<sup>a</sup>	<sup>a</sup>	<sup>a</sup>
1.0	18.1	18.2	(17.5)	19.5	18.0
2.5	19.4	19.4	17.4	19.6	18.3
5.0	19.4		17.8	19.6	18.9

<sup>a</sup>Means not detectable by SAXS.

reported previously for PEO/Li<sup>+</sup>-exchanged Laponite nanocomposites [3]. The absence of an organic modifier in the intergallery spacing of the clay is considered the main reason for the limited increase of the intergallery opening. It has been reported [4,20] that increasing the matrix molar mass facilitates the intercalation/exfoliation process. Increasing the molar mass implies a simultaneous increase of the matrix melt viscosity, which consequently leads to higher shear forces during melt mixing. However, from Fig. 8(b) and Table 3, it can be seen that the HMW PEO/pure Laponite nanocomposites display a diffraction peak positioned at a similar basal spacing as the LMW nanocomposites. This observation is again in good agreement with earlier reported results for PEO/Cloisite Na<sup>+</sup> nanocomposites [4]. It can thus be concluded that not only viscosity effects are important, but also the chemical compatibility between the polymer and the clay needs to be sufficiently high for an improved intercalation/exfoliation process to take place [20,21]. Hence, the presence of an organic modifier proves to be crucial for the PEO/pure Laponite nanocomposites, as this would improve the compatibility between PEO and the silicate clay layers.

Based on the previous section discussing the modified Laponite clays, component A/a, C/c and E/e are selected to modify Laponite in order to subsequently prepare LMW PEO/clay nanocomposites. The used modifier concentration equals 3 CEC and the clays are prepared at room temperature. Fig. 9(a)–(c) presents the SAXS diffraction spectra of the different PEO/modified Laponite nanocomposites.

The nanocomposites, based on modifier a, display no clearly detectable diffraction peak at lower silicate loadings. For silicate concentrations  $\geq 2.5$  wt%, a small peak with a very weak intensity can be detected. In our previous publication concerning PEO/Cloisite 30B nanocomposites [4], we discussed the existence of a threshold level for the silicate concentration ( $\sim 2.5$  wt%) above which no longer complete exfoliation can be expected. In view of the present results, this may suggest that the PEO/Laponite containing modifier a (PEO/Lap-mod a) nanocomposites tend to lead to an exfoliated structure at the lower silicate loadings. The SAXS spectra of the PEO nanocomposites based on modifier c and e display a more clearly observable diffraction peak, irrespective of the silicate concentration. From Table 3 it follows that the basal spacing of these nanocomposites is similar, or slightly higher, when compared with the basal spacing of their respective modified clay. The basal spacing varies between 17.4 and 19.6 Å, which is the range commonly reported for PEO intercalates with ‘less compatible’ clays [1,4,11]. Rather than inducing a further increase of the intergallery spacing, it appears that the PEO chains are sufficiently accommodated to intercalate in the existing spacing between the modified silicate layers. The modifier is believed to have facilitated the entry due to its polar nature, although this remains unproven.

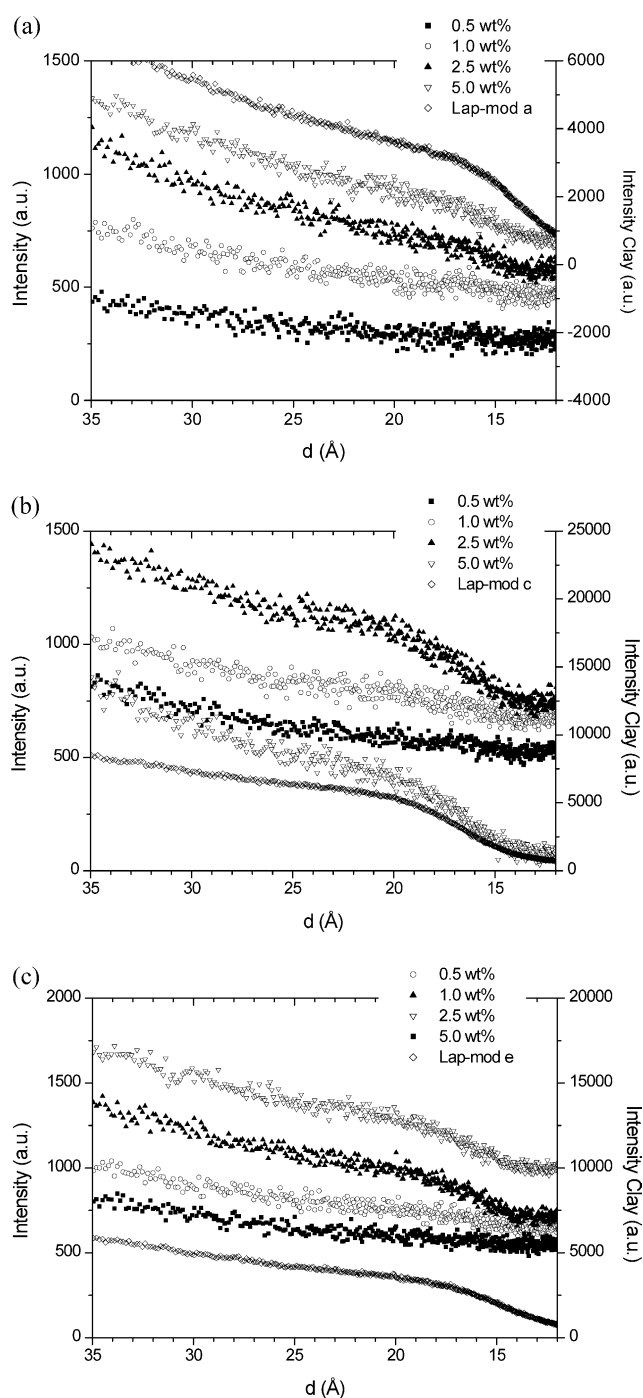


Fig. 9. SAXS diffraction spectra of the LMW PEO/modified Laponite nanocomposites. The Laponite is modified at 25 °C with 2 CEC of modifier a (a); modifier c (b) and modifier e (c). The right Y-axis corresponds to the respective modified Laponite clay. The curves of the nanocomposites have been shifted in the Y-direction for clarity.

It can be stated that the ion-dipole modification route appears to be less effective compared to the cation exchange modification. In the latter, the exchanged cations remain positioned at the silicate surface and provide the necessary compatibility whilst keeping the energetic balance of the clay crystal structure. This is not the case for the ion-dipole

route where part of the modifier could be expelled from the intergallery area upon intercalation of the polymer, significantly decreasing the envisaged compatibilisation.

### 3.2.2. Mechanical properties

The influence of the addition of clay on the mechanical properties is discussed as a function of the silicate concentration, modifier type and matrix molar mass. Fig. 10 features the shear storage modulus as a function of temperature for LMW and HMW PEO and their respective nanocomposites with pure Laponite. To evaluate the real contribution of the clay dispersion, the ratio between the shear storage modulus of the nanocomposite ( $G'_{\text{nano}}$ ) and the shear storage modulus of the respective PEO matrix ( $G'_{\text{PEO}}$ ) needs to be evaluated. Table 4 accordingly presents the calculated ratios for the respective PEO/pure Laponite nanocomposites. It follows that at low temperatures, below the glass-transition temperature ( $T_g$ ) of PEO, the nanocomposites display a similar to slightly lower stiffness compared to their respective PEO matrix. This is the result of a low relative modulus combined with a possible decrease of the matrix crystallinity in the presence of clays (see below), resulting in the apparent similarity of the respective storage moduli. At temperatures above the matrix  $T_g$  (e.g. 20 °C), the nanocomposites display a higher shear storage modulus than the one of the respective PEO. The actual increase is rather limited and dependent on the added silicate concentration. The strongest increase is observed for the HMW PEO/Laponite nanocomposites.

Fig. 11 presents the shear storage modulus as a function of temperature for the LMW PEO/modified Laponite nanocomposites and Table 5 provides the calculated ( $G'_{\text{nano}}/G'_{\text{PEO}}$ ) ratio. In correspondence to the previous results, the storage moduli at temperatures below  $T_g$  are similar, or lower, than the one of pure PEO. A crossover can be observed at higher temperatures. Consequently, the

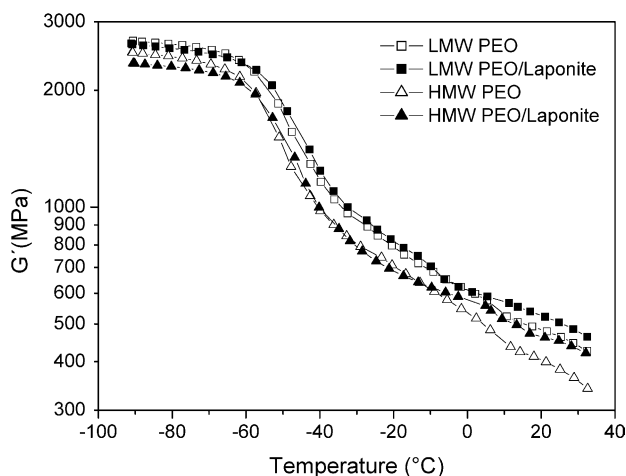


Fig. 10. Shear storage modulus ( $G'$ ) of LMW and HMW PEO and their respective nanocomposites with pure Laponite (2.5 wt%) as a function of temperature.

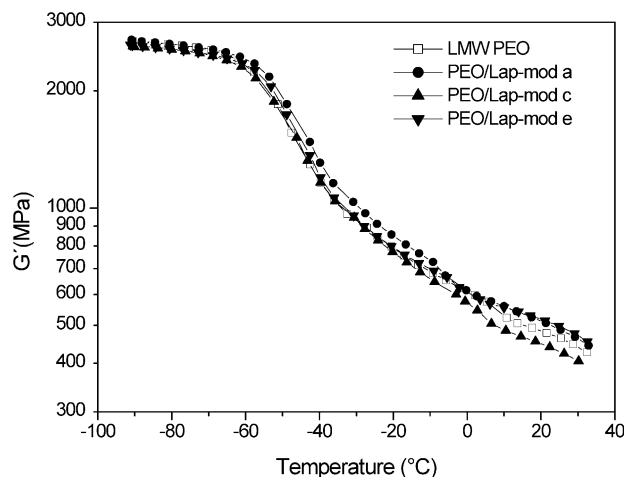


Fig. 11. Shear storage modulus ( $G'$ ) of various LMW PEO/modified Laponite nanocomposites (i.e. modifier a; modifier c and modifier e) (2.5 wt% silicate) as a function of temperature.

modulus of the nanocomposites at temperatures above  $T_g$  is higher than the modulus of PEO, although the increase is rather limited. The PEO/Lap-mod e nanocomposites display the strongest rise of the shear storage modulus. The nanocomposites based on Laponite modified with component c, display distinctly lower values at temperatures above  $T_g$ .

It is now very interesting to compare the  $G'$  values of the present nanocomposites with those of our previously studied PEO nanocomposites based on various Cloisite clays [4]. Fig. 12 summarises the ( $G'_{\text{nano}}/G'_{\text{PEO}}$ ) ratios for all examined LMW PEO nanocomposites as a function of the silicate concentration. The Cloisite clays include the natural montmorillonite Cloisite Na<sup>+</sup> and two organically modified clays, namely Cloisite 20A (apolar modifier) and Cloisite

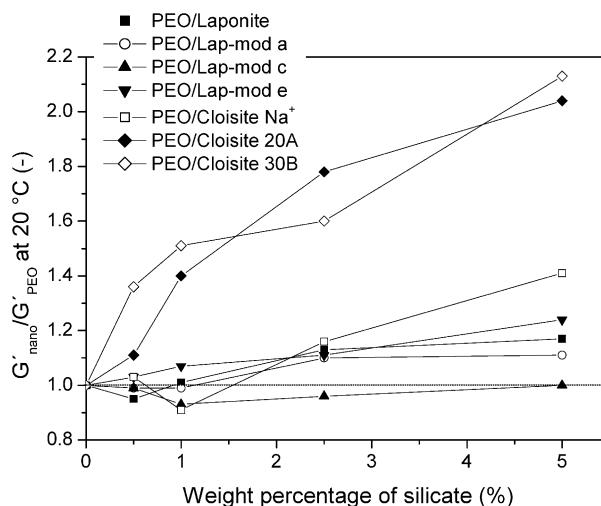


Fig. 12. Ratio between the shear storage modulus of the nanocomposite and the shear storage modulus of the LMW PEO matrix ( $G'_{\text{nano}}/G'_{\text{PEO}}$ ) as a function of the silicate concentration, both for the presently studied PEO/Laponite (pure and modified) nanocomposites, and previously studied PEO/Cloisite nanocomposites [4].



Table 4

Ratio between the shear storage modulus of the Laponite based nanocomposite and the shear storage modulus of the respective PEO matrix ( $G'_{\text{nano}}/G'_{\text{PEO}}$ ) at different weight percentages of silicate at  $-80^\circ\text{C}$  and  $20^\circ\text{C}$

Silic conc. (wt%)	LMW PEO/Laponite RD		HMW PEO/Laponite RD	
	$-80^\circ\text{C}$	$20^\circ\text{C}$	$-80^\circ\text{C}$	$20^\circ\text{C}$
0	1	1	1	1
0.5	0.94	0.95	1.06	1.23
1.0	0.97	1.01	1.05	1.22
2.5	1.01	1.13	0.98	1.21
5.0	0.98	1.17		

30B (polar modifier). It follows that the addition of pure Laponite, or any of the modified Laponite clays, does not result in the desired increase of the mechanical properties. The reason is twofold. Firstly, the resulting basal spacing increase upon intercalation is rather limited and comparable to those observed for the PEO/Cloisite  $\text{Na}^+$  nanocomposites. A strong increase of the basal spacing, or even exfoliation, of the silicate layers has been found to be essential for obtaining highly improved mechanical properties [4,15]. However, a second more structural reason needs to be taken into account. Based on their respective structure, it is important to note that the Cloisite clays and the Laponite clays have distinctly different aspect ratios. The supplier reports an aspect ratio ( $w/t$ ) of approximately 100 for the Cloisite clays, whereas the Laponite clays have a circular shape and an aspect ratio of about 25. Our previous research and reports in literature [4,15] have shown that the 'effective' aspect ratio of the dispersed silicate platelets is of significant importance. The PEO/Cloisite 20A and PEO/Cloisite 30B nanocomposites show a levelling of the shear storage modulus at higher silicate loadings. This was a direct result of ineffective clay dispersion leading to a decrease of the effective aspect ratio, and consequently the mechanical properties. This provides a structural base to explain the inability of the Laponite clays to lead to a strong increase of  $G'$  at temperatures above  $T_g$ . Using a modified

version of the Halpin–Tsai model, the effective aspect ratio of the respective dispersed clay can be evaluated. The model has been corrected for platelet reinforcement [15]:

$$\frac{G_{\text{nano}}}{G_{\text{m}}} = \frac{1 + \xi\eta V_{\text{f}}}{1 - \eta V_{\text{f}}} \quad (1)$$

with:

$$\eta = \frac{G_{\text{r}}/G_{\text{m}} - 1}{G_{\text{r}}/G_{\text{m}} + \xi} \quad (2)$$

$$\xi = \frac{w}{t} \quad (3)$$

$G_{\text{nano}}$ ,  $G_{\text{m}}$  and  $G_{\text{r}}$  are, respectively, the shear modulus of the nanocomposite, the matrix and the clay reinforcement.  $V_{\text{f}}$  is the volume concentration of the clay silicate and  $w/t$  is the aspect ratio of the added clay.

Fig. 13 presents the ( $G'_{\text{nano}}/G'_{\text{PEO}}$ ) of the different modified Laponite based nanocomposites, together with the Halpin–Tsai fitted values when assuming an aspect ratio of 25. As expected, the actual storage moduli are profoundly lower than expected on the basis of the fitting model. Although, the initial clay aspect ratio was already quite low, it can be concluded that the effective aspect ratio is even lower revealed by the profound overestimation of the model. Van Es [15] reported previously that a high effective aspect ratio was crucial for polyamide/Cloisite 20A nanocomposites to reach a high elastic modulus. Based on the formed nanostructures and the corresponding basal spacings of the presently examined nanocomposites, it can be concluded that the failure in obtaining sufficiently intercalated, or even exfoliated, structures as well as the low initial aspect ratio of the Laponite clay only resulted in minorly improved mechanical properties. Even the supposed exfoliated structure of the PEO/Lap-mod a nanocomposites is ineffective which originates from the maximum possible aspect ratio of the Laponite clay platelets.

Fig. 14(a)–(d) presents the shear loss modulus ( $G''$ ) as a function of temperature for the different LMW PEO nanocomposites. The  $T_g$  of PEO can be defined from the peak value. It can be seen that the  $T_g$  shifts towards higher temperatures upon the addition of clay for nearly all PEO/(modified/pure) Laponite nanocomposites. Only the

Table 5

Ratio between the shear storage modulus of the nanocomposite and the shear storage modulus of the LMW-PEO matrix ( $G'_{\text{nano}}/G'_{\text{PEO}}$ ) as different weight percentages of silicate for the different clay types at  $-80$  and  $20^\circ\text{C}$

Silic conc. (wt%)	Laponite-mod. a		Laponite-mod. c		Laponite-mod. e	
	$-80^\circ\text{C}$	$20^\circ\text{C}$	$-80^\circ\text{C}$	$20^\circ\text{C}$	$-80^\circ\text{C}$	$20^\circ\text{C}$
0	1	1	1	1	1	1
0.5	0.96	0.99	0.98	0.99	0.97	1.03
1.0	0.93	0.99	0.93	0.93	0.97	1.07
2.5	1.04	1.10	1.01	0.96	1.01	1.11
5.0	1.02	1.11	1.07	1.00	1.06	1.24

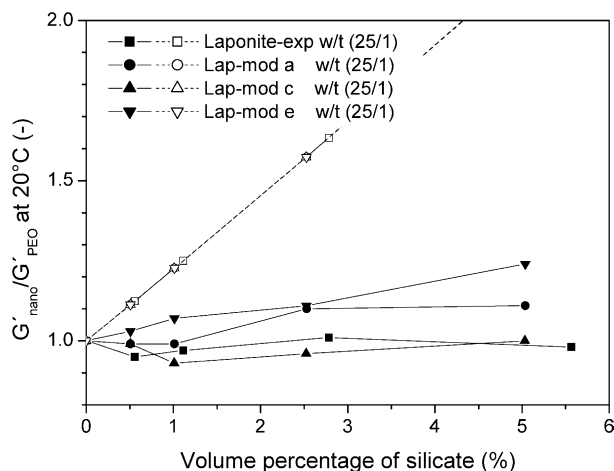


Fig. 13. Ratio between the shear storage modulus of the nanocomposite and the shear storage modulus of the PEO matrix ( $G'_{\text{nano}}/G'_{\text{PEO}}$ ) as a function of the silicate volume concentration for the LMW PEO/(modified or pure) Laponite nanocomposites (closed symbols). The open symbols represents the respective ( $G'_{\text{nano}}/G'_{\text{PEO}}$ ) value as predicted by the modified Halpin Tsai model for an aspect ratio of 25.

nanocomposites based on modifier c do not display this distinct shift. The shift in  $T_g$  is also reflected in the onset of the  $\tan \delta$  curve. An increase of the peak value in the  $G'$  curve corresponds to an increase of the onset of the  $\tan \delta$  curve. This is clearly shown by Fig. 15(a) and (b), which presents the  $\tan \delta$  curves for the PEO/Lap-mod c and PEO/Lap-mode nanocomposites, respectively. The increased  $T_g$  of the latter materials is visible by a shift of the  $\tan \delta$  onset. However, no shift can be observed for the PEO/Lap-mod c nanocomposites. The increased  $T_g$  values are commonly associated with a decreased mobility of the polymer chain between the silicate layers. Table 3 illustrates the limited intergallery spacing available for the PEO chains in between the Laponite clay layers. The SAXS spectra also revealed that the PEO/Lap-mod c nanocomposites possess a greater intergallery opening, which can be seen as more accommodating for the intercalated PEO chains. Considering the possible formation of a double layer of PEO chains in between the silicate layers [13], it seems logical that an increased spacing is more advantageous for the chain accommodation and mobility. The second relaxation peak visible at higher temperatures ( $\sim 15^\circ\text{C}$ ); both for pure PEO, as well as for the nanocomposites, can be assigned to intercrystalline effects [4,8,22]. It is also interesting to note that the  $\tan \delta$  curves return to the same level after passing the  $T_g$ . Only the nanocomposites based on modifier c show a marked influence of the addition of the clay as  $\tan \delta$  increases with an increasing silicate concentration.

In our previous publication, we reported that the  $\tan \delta$  level at peak position indicates the actual nanostructure present, whereby a strong decrease of the  $\tan \delta$  peak value is observed for highly intercalated (high  $\Delta d$ ) or exfoliated structures [4]. The PEO/(modified/pure) Laponite nanocomposites display no significant decrease of this value.

This confirms the observed SAXS results revealing limited intercalated nanostructures.

### 3.2.3. Crystallisation characteristics

To evaluate the influence of the clay addition on the crystallisation characteristics of the semi-crystalline PEO matrix, the most important thermal properties of the LMW PEO nanocomposites are summarised in Table 6. The crystallisation temperature ( $T_c$ ), as derived from the cooling run, is found to be only minorly influenced by the clay addition. Regardless of the clay type, the nanocomposites have  $T_c$ 's which are similar or, at higher clay concentrations, even slightly lower than the crystallisation temperature of pure PEO. Similar results have been reported previously for nanocomposites of PEO and various Cloisite clays ( $\text{Na}^+$ , 20A and 30B) [4]. In contrast to several literature reports [11,16], the present results indicate that the added clay does not act as a nucleating agent for crystallisation. The observed decrease of  $T_c$  at higher clay loadings even reveals that a higher degree of undercooling is needed to initiate PEO crystallisation.

The heat of fusion derived from the melting endotherms ( $\Delta H_m$ ), obtained from the first and the second heating run, displays a strong influence of the addition of clay. The PEO/pure Laponite nanocomposites show a marked decrease of the heat of fusion at lower silicate loadings ( $\leq 2.5$  wt%). At a silicate concentration of 5.0 wt%, however, the melt enthalpy displays a distinct increase, resulting in a value close the  $\Delta H_m$  of pure LMW PEO. A similar evolution of the melt enthalpy with silicate concentration has been observed previously for various PEO/Cloisite nanocomposites [4]. The reason for this apparent increase remains unclear. The  $\Delta H_m$  values of the nanocomposites based on the modified Laponite clays display an effect of both the applied modification and the clay concentration, although the trend is less pronounced. The PEO/Lap-mod a nanocomposites display a strong decrease of  $\Delta H_m$  at low clay concentrations, after which the heat of fusion is seen to increase, reaching similar values as the  $\Delta H_m$  of PEO. The nanocomposites based on modifier c and e display a decrease of the heat of fusion with the clay concentration, levelling off at 5.0 wt%. The melt temperature of the modified Laponite nanocomposites is highly comparable to the one of pure PEO. In contrast, the PEO/pure Laponite nanocomposites reveal a marked decrease of the melt temperatures at lower silicate loadings compared to the  $T_m$  of pure PEO. However, the  $T_m$  of the 5.0 wt% silicate nanocomposite has a  $T_m$  similar to PEO.

Based on the above results, it can be concluded that the addition of clay generally results in a decrease of the PEO crystallinity. The presence of clay is found to inhibit the crystal formation, although the lamellar thickness is quite constant, as can be concluded from the  $T_m$  values of the PEO/modified Laponite nanocomposites. More particularly, the PEO/pure Laponite nanocomposites reveal a substantial hindering of crystallisation at lower clay loadings,

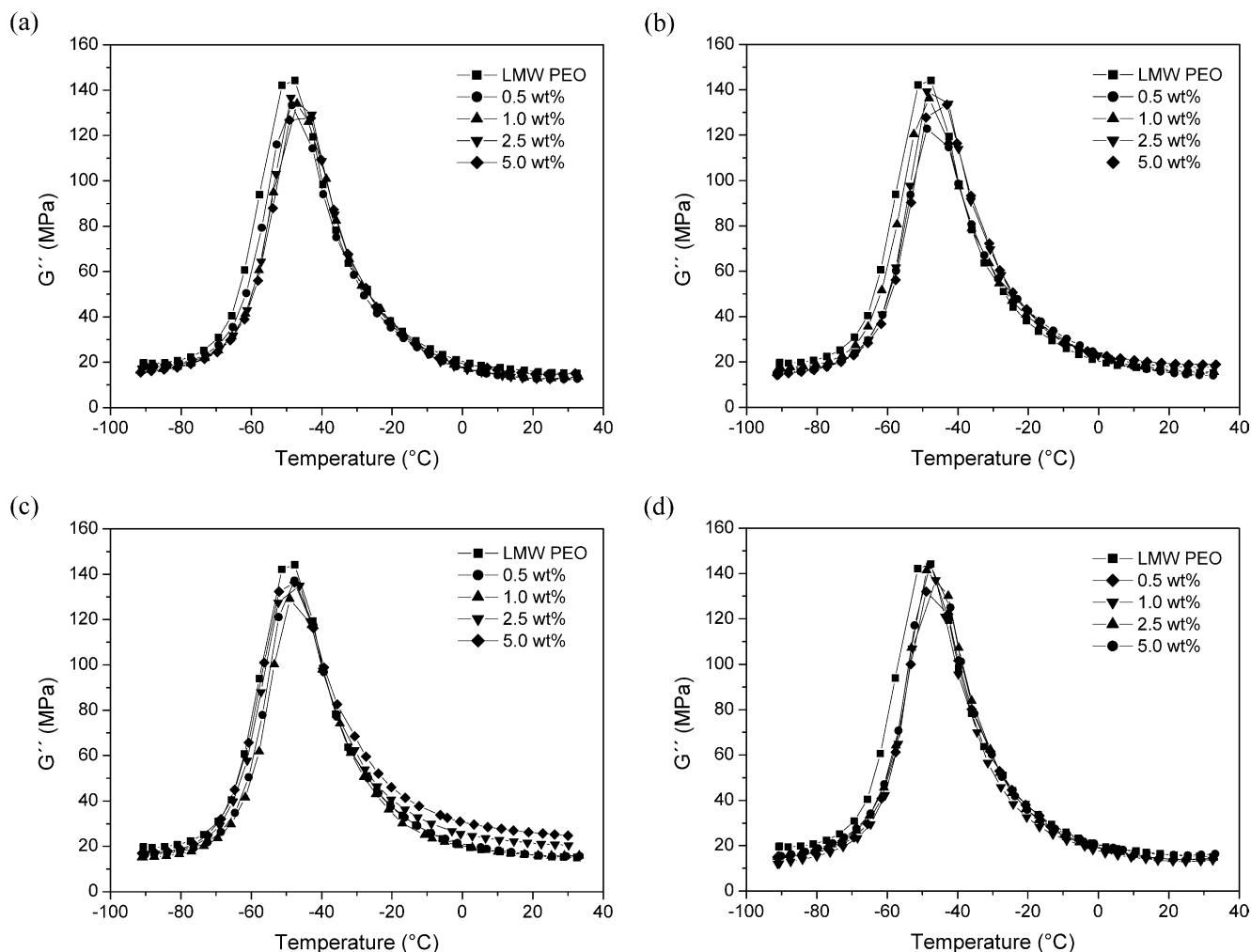


Fig. 14. Shear loss modulus as a function of temperature for various silicate concentrations for the following LMW PEO nanocomposites: (a) PEO/Laponite; (b) PEO/Lap-mod a; (c) PEO/Lap-mod c and (d) PEO/Lap mod e.

$\leq 2.5$  wt%, as manifested by a decreased  $\Delta H_m$ . This results in less perfect crystals with decreased lamellar thicknesses resulting in low values of  $T_m$ . The crystallisation inhibition in PEO/clay nanocomposites has been reported previously [4,11,23]. It is believed that the clay platelets restrict the chain mobility, which is confirmed by the increased glass-transition temperature (Fig. 14), hindering part of the polymer chains of entering the crystalline structure.

The chemical nature of the species present in the intergallery spacing of the clay also proves to be important. From the field of polymer electrolytes it is known that the presence of small cationic species, e.g.  $\text{Na}^+$ , has an inhibiting effect on the crystallisation of PEO as the polymer chain is reorganised towards the cations lowering the overall degree of crystallisation [11,24]. This appears to be coherent with the strongly decreased heat of fusions in the absence of an organic modifier in the intergallery spacing (PEO/pure Laponite nanocomposites). Upon the ion-dipole modification of the clay, the modifier is believed to, at least partly, shield the PEO chain from  $\text{Na}^+$  ion, reducing the effect of the latter on the PEO crystallisation.

This is reflected by the higher  $\Delta H_m$ 's for the nanocomposites based on the modified Laponite clays. In addition, this may indicate that part of the modifier remains located in the intergallery spacing upon PEO intercalation.

#### 3.2.4. Thermal stability

The influence of the clay addition on the thermal stability was studied with TGA under a  $\text{N}_2$  flow for the LMW PEO nanocomposites. Fig. 16 presents the weight loss as a function of temperature for the PEO/(modified/pure) Laponite nanocomposites having a silicate concentration of 2.5 wt%. Fig. 17 presents the onset decomposition temperature as derived from the TGA experiments as a function of the silicate concentration. From the presented results, it can be seen that the addition of clay has a beneficial effect on the thermal stability. The onset of decomposition is found to be influenced by the type of modifier and the silicate concentration. In addition, it can be stated that the temperature at 50% weight loss displays a similar trend and dependence as the onset temperature.

The addition of a low amount of modified Laponite clay

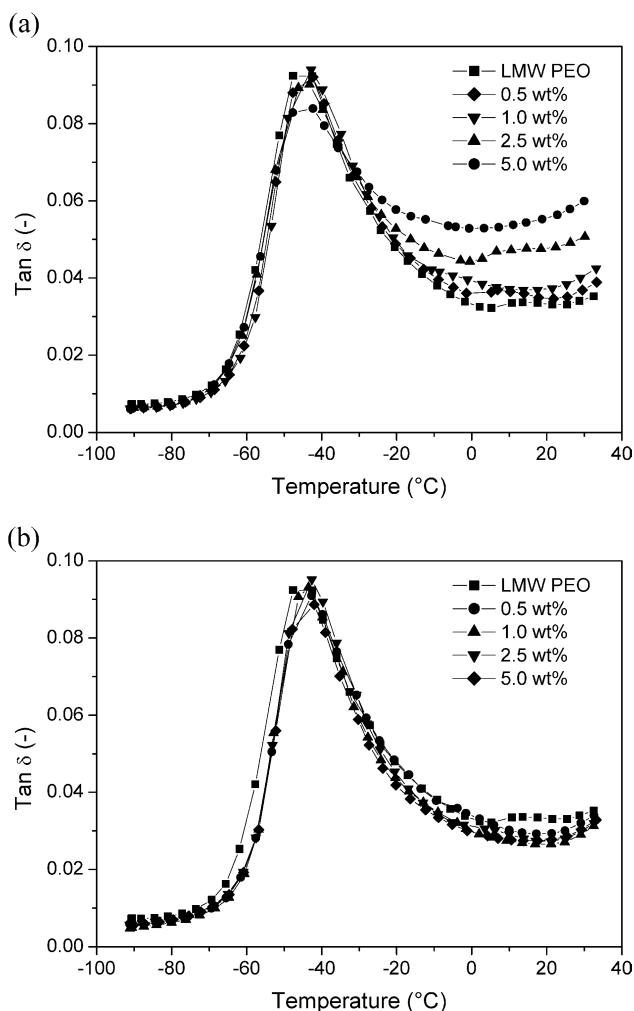


Fig. 15.  $\tan \delta$  as a function of temperature for the (a) PEO/Lap-mod c and (b) PEO/Lap-mod e nanocomposites for varying silicate concentrations.

(<2.5 wt%) results in a modest increase ( $\sim 10^\circ\text{C}$ ) of the decomposition temperature, regardless of the applied clay modification. In contrast, the pure Laponite based nanocomposites display decomposition temperatures similar to the one of pure PEO. Only at a silicate concentration of 5.0 wt%, a marked increase can be observed (Fig. 17). The silicate concentration is found to only weakly influence the decomposition temperature of the nanocomposites based on modifier C/c and E/e. The PEO/Lap-mod A/a nanocomposite, however, shows a distinct increase of the temperature at a silicate concentration of 5.0 wt%.

The influence of clay addition on the thermal stability is often assigned to the increased length of the pathway for the volatile degradation products [14,25,26]. It is furthermore believed that the barrier effect increases during decomposition due to a reassembly of the silicate layers parallel to the surface. The increase of the decomposition temperature for the present nanocomposites is rather limited when compared to other polymeric nanocomposites [14]. A similar low increase has been observed previously for nanocomposites of PEO and various Cloisite clays [4]. This

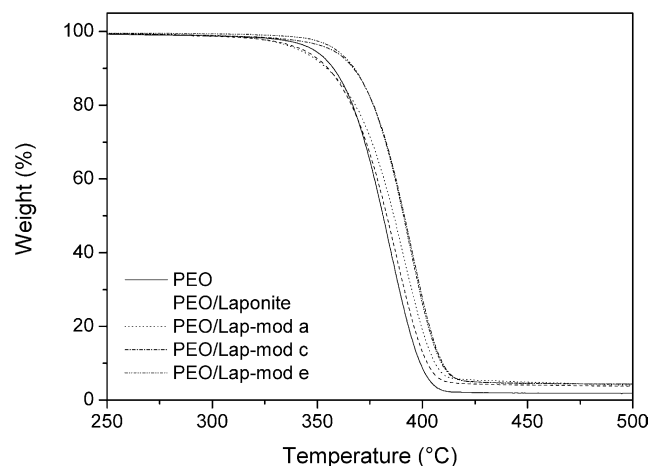


Fig. 16. TGA response of the LMW PEO/(modified or pure) Laponite nanocomposites having a silicate concentration of 2.5 wt%.

can be attributed to the difference in actual degradation mechanism of the different polymers and the possible specific interactions between PEO and the clay material [25]. The distinct difference between the pure Laponite nanocomposites and those based on the modified clays, especially at low silicate loadings, appears not to be related to the intergallery spacing between silicate layers. The presence of the (decomposed) modifier between the silicate layers may provide an additional hindrance for the volatile decomposition products of PEO to diffuse. The increased temperature for the pure Laponite and the Lap-mod A/a based nanocomposites at higher silicate loadings is probably related to structural effects. The silicate layers seem to provide a better barrier at a higher silicate concentration. When comparing the results of the PEO/(pure) Laponite nanocomposites with those of the corresponding PEO/Cloisite  $\text{Na}^+$  nanocomposites [4], the latter display higher decomposition temperatures (silicate concentration  $\leq 2.5$  wt%). It is thought that the lower aspect ratio of the

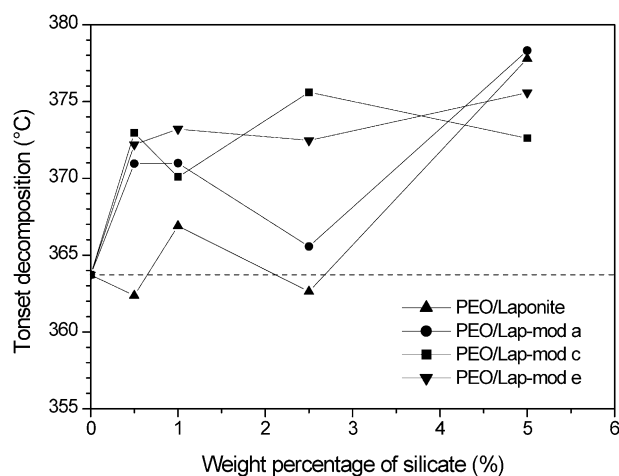


Fig. 17. Onset temperatures of the PEO decomposition as a function of the silicate concentration for the LMW PEO/(modified or pure) Laponite nanocomposites.

Table 6  
Thermal characteristics determined via DSC measurements of the different LMW PEO nanocomposites at various silicate concentrations

Silicate concentration (wt%)	First heating		Cooling, $T_{c,onset}$ (°C)	Second heating	
	$\Delta H_{m1}$ (J/g PEO)	$T_{m1,onset}$ (°C)		$\Delta H_{m2}$ (J/g PEO)	$T_{m2,onset}$ (°C)
LMW PEO	$168.5 \pm 3.0$	$59.8 \pm 1.2$	$52.0 \pm 0.2$	$161.6 \pm 3.6$	$58.3 \pm 2.3$
Laponite RD					
0.5	160.2	59.0	51.9	150.9	54.1
1.0	163.8	60.1	52.1	153.9	55.8
2.5	161.0	59.8	51.2	149.9	55.7
5.0	169.9	61.0	50.8	158.8	59.1
Lap-mod a					
0.5	166.5	62.3	51.9	155.4	58.7
1.0	163.7	61.7	52.0	155.6	59.0
2.5	171.6	62.3	52.1	159.6	60.0
5.0	173.1	60.5	51.2	162.7	59.2
Lap-mod c					
0.5	168.0	62.8	52.0	158.4	59.3
1.0	166.9	61.6	51.4	156.8	56.5
2.5	161.4	61.5	51.6	150.9	59.4
5.0	165.1	61.6	50.8	153.6	58.8
Lap-mod e					
0.5	165.9	61.8	52.3	160.1	59.8
1.0	165.4	62.5	51.7	157.3	56.8
2.5	164.5	61.1	51.4	155.0	58.2
5.0	165.1	62.8	50.6	157.6	58.8

Laponite clay is less efficient in providing a good barrier. At a higher silicate concentration, this effect appears to be minimised, probably due to overlapping clay platelets.

#### 4. Conclusions

It was possible to organically modify Laponite clay with low molar mass PEG's. The temperature of modification proved to be less important, providing means for the clay to be easily modified at room temperature in a non-oxidative environment. Based on the obtained basal spacings, the following order of efficiency of the different modifiers could be established: poly(ethylene glycol) methyl ether (C/c) > tetraethylene glycol dimethyl ether (E/e) > 4,7,10-trioxal-1,13-tridecanediamine (A/a) > poly(ethylene glycol) (B/b) > poly(ethylene glycol)bis(carboxy methyl)ether (D/d). It is believed that the modifier is present in a non-crystalline, double layer conformation for modifier A/a, B/b and E/e. Modifier C/c is present in an intermediate conformation, pending between a 'bilayer' and a 'trilayer', or paraffin-type of organisation. The modified clays displayed good thermal stability at the nanocomposite processing temperature.

The PEO nanocomposites based on pure Laponite, as well as the modified Laponite nanocomposites (modifier A/a, C/c and E/e), display only a very minor improvement of the mechanical properties, irrespective of the PEO molar mass. The reason was found to be twofold. The initial aspect ratio of the Laponite clay is low,  $w/t=25$ , and the obtained basal spacing increase were very limited ( $\Delta d=6.8-9.6 \text{ \AA}$ ). It can be concluded that the effective aspect ratio of the

dispersed clay is too low to provide the desired improvement of the mechanical properties. The applied organic modification does not result in a better intercalation/exfoliation process. It can be concluded that the ion-dipole modification route provides a less effective modification when compared to the cation exchange modification.

The addition of clay to semi-crystalline PEO does not lead to a nucleation of the PEO crystallisation. In contrast, it was found that the clay inhibits the crystallisation resulting in decreased heat of fusions. The effect is the strongest for the pure Laponite nanocomposites and is attributed to the presence of the  $\text{Na}^+$  ions. In the presence of a modifier is believed to shield the PEO from the interfering cations. The nanocomposites based on the modified Laponite have an increased thermal stability at very low clay loadings, whereas the stability of the PEO/pure Laponite nanocomposites was only improved at higher silicate concentrations.

#### Acknowledgements

The authors wish to thank Katarina Flodström of the Department of Physical Chemistry 1 of Lunds University for the use of the SAXS apparatus, as well as for the guidance and discussions.

#### References

- [1] Jacob MME, Hackett E, Giannelis EP. *J Mater Chem* 2003;13:1–5.
- [2] Aranda P, Ruiz-Hitzky E. *Acta Polym* 1994;45:59–67.
- [3] Doeff M, Reed JS. *Solid State Ionics* 1998;113–115:109–15.

- [4] Loyens W, Jannasch P, Maurer FHJ. *Polymer* 2005, this issue.
- [5] Lim SK, Kim JW, Chin I, Kwon YK, Choi HJ. *Chem Mater* 2002;14:1989–94.
- [6] Shen Z, Simon GP, Cheng Y-B. *Polymer* 2002;43:4251–60.
- [7] Labbe P, Reverdy G. *Langmuir* 1988;4:419–25.
- [8] Alexandre M, Dubois P, Sun T, Garces JM, Jerome R. *Polymer* 2002;43:2123–32.
- [9] Muzny CD, Butler BD, Hanley HJM, Tsvetkov F, Peiffer DG. *Mater Lett* 1996;28:379–84.
- [10] Chen W, Xu Q, Yuan RZ. *Mater Sci Eng B* 2000;77:15–18.
- [11] Strawhecker KE, Manias E. *Chem Mater* 2003;15:844–9.
- [12] Harris DJ, Bonagamba TJ, Schmidt-Rohr K. *Macromolecules* 1999;32:6718–24.
- [13] Hackett E, Manias E, Giannelis EP. *Chem Mater* 2000;12:2161–7.
- [14] Alexandre M, Dubois P. *Mater Sci Eng* 2000;28:1–63.
- [15] Van Es M. PhD Thesis. TUDelft, The Netherlands; 2001.
- [16] Fornes TD, Paul DR. *Polymer* 2003;44:3945–61.
- [17] Vaia RA, Teukolsky RK, Giannelis EP. *Chem Mater* 1994;6:1017–22.
- [18] Hackett E, Manias E, Giannelis EP. *J Chem Phys* 1998;108:7410–5.
- [19] Li Y, Ishida H. *Chem Mater* 2002;14:1398–404.
- [20] Fornes TD, Yoon PJ, Keskkula H, Paul DR. *Polymer* 2001;42:9929–40.
- [21] Dennis HR, Hunter DL, Chang D, Kim S, White JL, Cho JW, Paul DR. *Polymer* 2001;42:9513–22.
- [22] Boyd RH. *Polymer* 1985;26:323–47.
- [23] Ogata N, Kawakage S, Ogihara T. *Polymer* 1997;38:5115–8.
- [24] Edman L, Ferry A, Doeff MM. *J Mater Res* 2000;15:1950–4.
- [25] Zhao Q, Samulski ET. *Macromolecules* 2003;36:6967–9.
- [26] Zanetti M, Kashiwagi T, Falqui L, Camino G. *Chem Mater* 2002;14:881–7.